AGU PUBLICATIONS

JGR

Journal of Geophysical Research: Oceans

RESEARCH ARTICLE

10.1002/2014JC010352

Key Points:
- Florida Bay seagrass meadows were net autotrophic across a productivity gradient
- Eddy covariance measured the most accurate and high-resolution flux rates
- Stratification and sensor precision limited the Eulerian control volume accuracy

Correspondence to:
M. H. Long,
mlong@whoi.edu

Citation:
Long, M. H., P. Berg, and J. L. Falter (2015), Seagrass metabolism across a productivity gradient using the eddy covariance, Eulerian control volume, and biomass addition techniques, *J. Geophys. Res. Oceans*, *120*, 3624–3639, doi:10.1002/2014JC010352.

Received 29 JUL 2014
Accepted 21 APR 2015
Accepted article online 25 APR 2015
Published online 22 MAY 2015

Seagrass metabolism across a productivity gradient using the eddy covariance, Eulerian control volume, and biomass addition techniques

Matthew H. Long[1,2], Peter Berg[1], and James L. Falter[3,4]

[1]Department of Environmental Sciences, University of Virginia, Charlottesville, Virginia, USA, [2]Now at Department of Marine Chemistry and Geochemistry, Woods Hole Oceanographic Institution, Woods Hole, Massachusetts, USA, [3]Australian Research Council Centre of Excellence for Coral Reef Studies, University of Western Australia, Western Australia, Australia, [4]Oceans Institute, University of Western Australia, Western Australia, Australia

Abstract The net ecosystem metabolism of the seagrass *Thalassia testudinum* was studied across a nutrient and productivity gradient in Florida Bay, Florida, using the Eulerian control volume, eddy covariance, and biomass addition techniques. In situ oxygen fluxes were determined by a triangular Eulerian control volume with sides 250 m long and by eddy covariance instrumentation at its center. The biomass addition technique evaluated the aboveground seagrass productivity through the net biomass added. The spatial and temporal resolutions, accuracies, and applicability of each method were compared. The eddy covariance technique better resolved the short-term flux rates and the productivity gradient across the bay, which was consistent with the long-term measurements from the biomass addition technique. The net primary production rates from the biomass addition technique, which were expected to show greater autotrophy due to the exclusion of sediment metabolism and belowground production, were 71, 53, and 30 mmol carbon m^{-2} d^{-1} at 3 sites across the bay. The net ecosystem metabolism was 35, 25, and 11 mmol oxygen m^{-2} d^{-1} from the eddy covariance technique and 10, −103, and 14 mmol oxygen m^{-2} d^{-1} from the Eulerian control volume across the same sites, respectively. The low-flow conditions in the shallow bays allowed for periodic stratification and long residence times within the Eulerian control volume that likely reduced its precision. Overall, the eddy covariance technique had the highest temporal resolution while producing accurate long-term flux rates that surpassed the capabilities of the biomass addition and Eulerian control volume techniques in these shallow coastal bays.

1. Introduction

Seagrass ecosystems have been identified as an important sink for atmospheric carbon through the burial of organic matter [*Duarte et al*., 2010; *Fourqurean et al*., 2012]. On average, two thirds of the carbon stored in seagrasses is in the belowground biomass [*Fourqurean et al*., 2012] and this belowground storage contributes significantly to the ability of seagrass meadows to be net autotrophic [*Duarte et al*., 2010]. However, the majority of seagrass productivity studies have focused on the physiology and growth of aboveground seagrass biomass [*Duarte and Chiscano*, 1999]. In contrast to this monotypic view, seagrass meadows represent diverse communities of autotrophic and heterotrophic organisms living both aboveground and belowground. Therefore, it is important to make community-scale and ecosystem-scale measurements of net metabolic fluxes in order to incorporate all of the metabolic components in seagrass meadows and properly evaluate their ability to act as a net sink for carbon dioxide.

Many studies have investigated the long-term productivity of seagrasses over a wide range of conditions, but the techniques used (such as seagrass biomass addition techniques) [e.g., *Zieman*, 1974] are time consuming, destructive, and do not include belowground production nor sediment metabolism [*Kemp et al*., 1990]. The seagrass biomass addition or marking technique involves the measurement of aboveground biomass that is added over time by marking the seagrass shoots, collecting the aboveground biomass, and separating the biomass by growth before and after the mark [*Zieman*, 1974]. The biomass addition technique integrates over long-time periods (typically weeks) and therefore makes it difficult to examine how seagrass metabolism responds to rapidly changing environmental conditions. For example, the metabolism of seagrasses has been

shown to be controlled by light and water motion [*Thomas and Cornelisen*, 2003; *Mass et al*., 2010; *Hume et al*., 2011]; factors that can vary on time scales ranging from minutes to hours as well as weeks to months due to everchanging weather and climate conditions. In order to separate short-term physiological responses from long-term physiological changes, it is useful to examine these variables and the interactions between them at the greatest possible temporal resolution. Furthermore, higher sampling frequencies allow for greater data density and, therefore, the ability to measure independent rates of seagrass metabolism over a wider variety of environmental conditions within the same period of study. Therefore, the application of techniques that measure at a fast rate under in situ conditions is advantageous to determine how the metabolism of seagrass communities responds to rapidly changing environmental conditions.

The Eulerian control volume technique [*Falter et al*., 2008] and the eddy covariance (EC) technique [*Berg et al*., 2003] are two such methods that can measure rates of seagrass ecosystem metabolism under in situ conditions at relatively high temporal resolution (hours or less). The Eulerian technique consists of a control volume where the changes in solute concentrations, current magnitude, and current direction are determined across a finite volume to determine the net solute mass transfer through the control volume [*Genin et al*., 2009; *Monismith et al*., 2010; *Teneva et al*., 2013]. The Eulerian control volume approach has the advantages of integrating over very large areas, including metabolism in the water column, and being nonintrusive [*Falter et al*., 2008]. However, the Eulerian technique must be deployed over many diel cycles to determine accurate net metabolic rates because it suffers from error and signal loss caused by depth and/or flow limitations, difficulties in determining the air-water oxygen (O_2) exchange at very high or very low O_2 saturation, and rapid changes in flow and light [*Atkinson and Grigg*, 1984; *Ziegler and Benner*, 1998; *Falter et al*., 2008].

The eddy covariance (EC) technique determines the exchange of O_2 between benthic communities and the overlying water by correlating instantaneous changes in the vertical velocity and the O_2 concentration and integrating the product of these variations over time [*Berg et al*., 2003]. The in situ EC technique has the advantages of a high temporal resolution ($<$1 h), the capacity to integrate over large areas (10s-100s m^2), and the adaptability to a variety of different benthic systems [*Berg et al*., 2003; *Hume et al*., 2011; *Long et al*., 2013]. The EC technique has been validated and compared to benthic chambers [*Berg et al*., 2003, 2013] and microprofiling measurements [*Brand et al*., 2008; *Berg et al*., 2009] and has shown a higher resolution and accuracy than these standard methods. While the EC method has proven to be a large improvement over traditional measurements, it requires significant data processing to avoid potential errors due to coordinate rotation [*Baldocchi*, 2003; *Lorke et al*., 2013], sensor malfunction [*Long et al*., 2013; *Berg et al*., 2013], and changes in O_2 storage within the water column [*Rheuban et al*., 2014; *Long et al*., 2015].

In this study, we compare the biomass addition technique, the Eulerian control volume technique, and the EC technique to examine seagrass ecosystem metabolism across a nutrient and productivity gradient in Florida Bay. We then compare differences in the resolution and accuracy of these methods as well as what they can tell us about the in situ metabolism of seagrass ecosystems measured at different temporal and spatial scales.

2. Methods

2.1. Study Site

The study site for this research was the shallow estuary of Florida Bay, Florida, USA during July and August of 2012. Three sites were chosen across a productivity and nutrient gradient, with the lowest amounts of seagrass biomass, sediment organic matter, and sedimentary total phosphorus present in the northeast and the highest amounts in the southwest [*Zieman*, 1989; *Fourqurean and Zieman*, 2002, *Long et al*., 2008]. Each site was selected to have monotypic beds of the seagrass *Thalassia testudinum* at Duck Key (25° 10′ 36.60" N, 80° 29′ 20.52" W), Bob Allen Keys (25° 2′ 9.27" N, 80° 41′ 10.66" W), and Rabbit Key Basin (24° 58′ 4.89" N, 80° 50′ 19.80" W) (Figure 1). Sites were chosen to have similar depths (1.7–1.9 m average depth) and a consistent and homogenous benthic community within a ~200 m radius surrounding the site.

2.2. Eulerian Control Volume

The Eulerian technique consisted of an equilateral, triangular control-volume [*Falter et al*., 2008] with the EC instrumentation (including a velocimeter) at its center. At each site, a control volume was established with 250 m long sides and a miniDO$_2$T O_2 optode and temperature logger (PME, USA) at each apex at the same height as the EC measuring volume (0.35–0.55 m). The O_2 optodes were calibrated individually in the

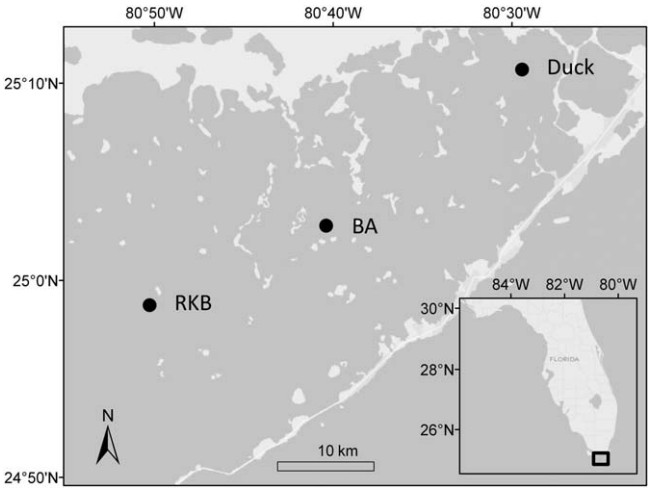

Figure 1. Locations of Rabbit Key Basin (RKB), Bob Allen Keys (BA), and Duck Key (Duck) in Florida Bay at the Southern tip of Florida, USA.

laboratory, corrected for in situ salinity and temperature, and intercalibrated before and after each site change (every 3–4 days) by placing them together in a sealed bucket of ambient seawater to account for any sensor drift. The Eulerian control volume was deployed for 5, 3, and 6 × 24 h periods at RKB, BA, and Duck, respectively. The Eulerian method was used only to provide an alternative, comparative measure for the EC technique, and therefore was deployed about half of the time over which EC fluxes were determined. A logarithmic velocity profile above the static seagrass canopy height, assuming a dense canopy that limits within-canopy flow [*Nepf*, 2012], was used to model vertical current profiles and depth-integrated transport from the point measurements of velocity made at depth. Total water depth was determined from the pressure sensor on the velocimeter.

The O_2 metabolism within the control volume was determined from a differential form of the advection-dispersion-reaction equation composed of a local accumulation term, the *x* and *y* horizontal flux components, and the flux of O_2 across the air-water interface derived by *Falter et al*. [2008] in the equation:

$$Flux = \langle \frac{\partial C}{\partial t} \cdot h \rangle + \langle q_x \rangle \cdot \langle \frac{\partial C}{\partial x} \rangle + \langle q_y \rangle \cdot \langle \frac{\partial C}{\partial y} \rangle - \langle J_{gas} \rangle \quad (1)$$

where the $\langle\rangle$ indicates spatial averaging over the control volume, C is the O_2 concentration, t is time, h is the tidally-varying water column height, q_x and q_y are the depth-integrated lagrangian transport terms in the longitudinal and transverse directions, and J_{gas} is the flux across the air-water interface [see *Falter et al*., 2008].

The relative position and concentration at each of the apices was used to define a surface with the form: $n_x x + n_y y + n_c C = \text{constant}$. These coefficients ($n_x$, n_y, n_c) were then used to calculate the gradients $\partial C/\partial x$ and $\partial C/\partial y$ [see *Falter et al*., 2008, equations (7)–(10) for more details]. The J_{gas} flux component was determined from the product of the O_2 gas exchange coefficient (k) and the difference between the 100 % saturation O_2 concentration at a given temperature and salinity and the ambient water O_2 concentration [*Broecker and Peng*, 1982]. The gas exchange coefficient was calculated from the wind velocities normalized to a 10 m height (u) by the equation: $k = 1.58e^{0.30u}$, as defined by *Raymond and Cole* [2001] for estuarine systems. Wind data was obtained from the National Data Buoy Center at the center of Florida Bay (Whipray Basin).

Daily rates of net ecosystem metabolism (NEM), gross primary production (GPP), and respiration (R) were determined from complete 24 h data series with the flux rates weighted by the hours of light and dark [*Falter et al*., 2008; *Hume et al*., 2011]. Due to the inability to separate respiration from gross photosynthetic production in the net flux, the nighttime and daytime respiration rates were assumed to be the same [*Cole et al*., 2000; *Falter et al*., 2008; *Hume et al*., 2011]. The seagrass NEM rates were converted using a simple, first-order 1:1 ratio between O_2 and carbon [*Ziegler and Benner*, 1998; *Duarte et al*., 2010] to allow for the final comparison between the methods.

To further differentiate benthic from planktonic rates of metabolism derived from the control volume approach, water column metabolic rates were determined daily by incubating water column samples under ambient conditions in four replicate 0.6 L light and dark bottles at each site across the study period. The rates of O_2 production or consumption were determined for ~ 4 h during midday from starting and end point measurements using an O_2 optode (Hach, USA). Sediment characteristics were evaluated in four sediment cores (0.1 m diameter x 0.3 m depth) at each site with the total sedimentary phosphorus determined by the persulfate digestion method [*Koroleff*, 1983].

2.3. Eddy Covariance

The EC instrument, deployment, and data analysis was designed and conducted as described by *Long et al.* [2015]. Briefly, the EC instrument used an Acoustic Doppler Velocimeter (Nortek AS, Norway) that was coupled to a fast-responding ($<$ 0.3 s) Clark-type O_2 microsensor [*Revsbech*, 1989] by a pA amplifier [*Berg et al.*, 2003; or *McGinnis et al.*, 2011]. It was deployed over 24 h periods to capture diel fluctuations with the measuring volume of the instrument at 0.35–0.55 m above the sediment surface, or approximately double the seagrass canopy height [see *Long et al.*, 2015; *Burba*, 2013]. The EC instrument sampled at 64 Hz and was limited to ~24 h deployments due to frequent sensor malfunction and fouling; the glass microsensors generally showed microbial fouling in the subtropical waters after 48 h in situ [*Long et al.*, 2013]. Sixteen individual EC deployments were conducted at each site that resulted in 7, 8, and 12 $\times$ 24 h data sets for Rabbit Key Basin (RKB), Bob Allen Keys (BA), and Duck, respectively. Data loss in 21 out of the 48 total deployments was due to sensor fouling by seagrass and algae, sensor malfunction, and breakage of the small glass sensors.

The velocity data were used to determine the current direction, mean current at depth, and significant wave height, or the average height of the highest third of waves [*Wiberg and Sherwood*, 2008]. Tidal flows resulted in a reversal of the current direction and low turbulence ~ twice daily and these periods were removed from analysis. A pressure sensor on the Velocimeter determined the water depth, wave height, and wave period using QuickWave software (Nortek, USA). A salinity logger (Onset, USA) and two Odyssey (Dataflow Systems, New Zealand) photosynthetically active radiation (PAR) sensors that were calibrated to a LI-COR 193SA Spherical PAR sensor (LI-COR, USA) as described in *Long et al.* [2012b] were also deployed during each sampling period. A vertical array of HOBO temperature sensors (Onset, USA) were deployed over a 2 week period at heights of 0.10, 0.35, 0.80. 1.25, and 1.70 m above the sediment surface and were intercalibrated between site changes every ~3 days.

The EC benthic O_2 flux was determined over 0.25 h intervals from the time-averaged product of the instantaneous variations in the vertical velocity and the O_2 concentration as described by *Berg et al.* [2003] using the software package EddyFlux (Peter Berg, unpublished). The instantaneous variations in the vertical velocity and O_2 concentration were determined by Reynolds Decomposition with the means determined from linear detrending over each 0.25 h interval. The data were carefully examined for sensor malfunction, corrected for the storage of O_2 in the water column [*Rheuban et al.*, 2014], and not sensitive to the rotation of the coordinate system [*Long et al.*, 2015]. The data were then averaged to hourly rates to compare with the Eulerian method. The daily rates of NEM, GPP, and R were calculated by the same method as the Eulerian rates above.

2.4. Biomass Addition

The net change in aboveground seagrass biomass over time (defined here as the Net Primary Production or NPP) was evaluated in four replicate quadrats (0.1 m $\times$ 0.2 m) at each site, which were randomly distributed within the area being measured by the EC system. Each seagrass short shoot (bundles of 3–7 blades) was marked by punching it through with a needle [*Zieman*, 1974]. Two weeks after punching, the aboveground seagrass material was collected and separated using the punch mark into newly grown biomass and old biomass, giving the NPP rates as well as the density and total seagrass biomass for each site. The seagrass leaves were freeze-dried, ground, and their carbon content determined on a Carlo-Erba elemental analyzer. The seagrass NPP in mmol C m^{-2} d^{-1} was determined from the product of the short shoots m^{-2}, the grams of new leaf material per short shoot over time, and the C content of the new leaf material. The differences between methods and across sites were evaluated by ANOVAs at a $p = 0.05$ with Tukey post tests to determine individual differences between sites.

3. Results

The productivity and nutrient gradients across Florida Bay [*Fourqurean and Zieman*, 1992, 2002] were well represented by the three sites across a gradient of increasing seagrass biomass, total sedimentary phosphorus concentrations, and sediment organic matter from the northeast site of Duck Key (Duck) to the southwest site of Rabbit Key Basin (RKB) (Table 1 and Figure 1). Water column O_2 production and consumption rates from bottle incubations showed a similar trend but were not significantly different across the sites and were on average an order of magnitude lower than the Eulerian and EC fluxes (Table 2). Temperature profiles indicated a well-mixed water column at the high velocity site of RKB and episodic stratification at the lower velocity sites of BA and Duck (Figure 2). At RKB, there was a predictable current velocity and direction

Table 1. Site Characteristics and ANOVAs Across Sites[a]

Site	Aboveground Biomass	Sediment Total Phosphorus	Water Column Temperature	Current Velocity	Significant Wave Height	Salinity
	g dry weight m^{-2}	μmol g^{-1}	°C	cm s^{-1}	cm	PSU
RKB	136 ± 35	2.9 ± 1.0	30.7 ± 1.4	5.0 ± 2.6	2.8 ± 1.9	36.4 ± 2.0
BA	75 ± 20	1.4 ± 0.6	29.1 ± 1.0	1.7 ± 0.6	3.1 ± 3.0	30.6 ± 1.0
Duck	24 ± 11	0.8 ± 0.2	31.2 ± 1.5	2.3 ± 1.1	3.1 ± 1.5	24.5 ± 2.1
F_2	15.14	49.77	135.01	187.68	2.63	255.01
p	0.0019	<0.0001	<0.0001	<0.0001	0.073	<0.0001

[a]The ± values are standard deviations. The current velocity is the depth-averaged flow velocity determined assuming a logarithmic profile above the seagrass canopy (see text).

(Figures 2d and 2e) and these tidal effects became less pronounced moving across Florida Bay toward the isolated site of Duck.

3.1. Eulerian Control Volume

The Eulerian flux rates had a much greater range than the EC rates and this range increased across the decreasing productivity gradient (Table 2, Figures 3 and 4), despite the similar irradiances over the time periods each method was conducted (Figure 3). The Eulerian method revealed a linear P-I relationship, rather than a typical saturating relationship, but showed reduced correlation coefficients, broader flux distributions, and larger 95% confidence intervals compared to that of the EC data (Figure 4). The slopes for the Eulerian P-I curves were similar to that of the EC slopes for the two most productive sites (i.e., Figures 4a and 4d, Figures 4b and 4e) but the slopes were very different for the lowest biomass site, Duck (Figures 4c and 4f). The time required for water to pass through the control volume, based on the average width of the triangular control volume and the average current velocities (Table 1), was on average 1.2, 3.5, and 2.6 h for RKB, BA, and Duck, respectively. Therefore, the Eulerian technique had a limited temporal resolution at the low current speed sites of BA and Duck, significantly reducing the amount of independent flux estimates generated at these sites (Figures 3e and 3f).

The Stokes drift velocity was calculated using the longest possible fetch and highest significant wave height (both occurring at Duck) to determine if wave propagation was influencing transport through the control volume in addition to the transport by the mean current velocities determined at depth. Given the significant wave height, water depth, and wave period of ~0.03 m, ~1.8 m, and ~4 s, respectively, the calculated Stokes drift velocity at Duck averaged just 0.13 ± 0.21 cm s^{-1} (mean ± standard deviation or SD) [see *Dean and Dalrymple*, 1991; *Monismith and Fong*, 2004]; speeds that were over an order of magnitude lower than the observed average current velocities (Figure 2d and Table 1). We expect that the Stokes drift would be even lower at Rabbit Key Basin and Bob Allen Key given their reduced fetch and wave heights relative to Duck. The average gas exchange coefficient (k) calculated over the sampling period was 4.73 ± 1.66 cm h^{-1} (mean ± SD, range = 2.69–10.97 cm h^{-1}) given average wind speeds of 3.6 m s^{-1} (range = 1.8–6.5 m s^{-1}); values consistent with prior studies of gas exchange in similar estuarine environments where k was calculated from both wind velocities (3–7 cm h^{-1}) [*Raymond and Cole*, 2001] and near-surface turbulence measurements (2.2–12.0 cm h^{-1}) [*Zappa et al.*, 2003]. The average difference between the O_2 optodes at each apex was 5.26 ± 8.84 μmol L^{-1} (± SD). The O_2 concentrations varied from ~ 146 to 245 μmol L^{-1} (75–131% saturation), 124–318 μmol L^{-1} (59–172 % saturation), and 152–315 μmol L^{-1} (71–160% saturation) at RKB, BA, and Duck, respectively.

Table 2. Metabolic Rates and ANOVAs Across Sites for Each Method[a]

	Eddy Covariance			Eulerian Control Volume			Water Column			Biomass Addition
	R	GPP	NEM	R	GPP	NEM	R	GPP	NEM	NPP
Site	mmol O_2 m^{-2} d^{-1}			mmol O_2 m^{-2} d^{-1}			mmol O_2 m^{-2} d^{-1}			mmol C m^{-2} d^{-1}
RKB	−155 ± 14	190 ± 27	35 ± 25	−239 ± 26	248 ± 24	10 ± 9	−16 ± 6	19 ± 5	3 ± 5	71 ± 9
BA	−127 ± 23	151 ± 23	25 ± 15	−344 ± 79	241 ± 37	−103 ± 43	−12 ± 4	16 ± 4	4 ± 4	53 ± 7
Duck	−52 ± 4	68 ± 6	11 ± 2	−233 ± 48	247 ± 40	14 ± 21	−10 ± 3	10 ± 7	0.5 ± 2	30 ± 14
F_2	17.1601	14.4724	0.4547	1.3859	0.0082	7.6119	0.2715	0.1511	0.0651	2.6289
p	<0.0001	<0.0001	0.6398	0.2847	0.9918	0.0065	0.7672	0.8617	0.9374	0.1326

[a]Standard errors (± values) were used to compare error estimates between the high-resolution and low-resolution techniques.

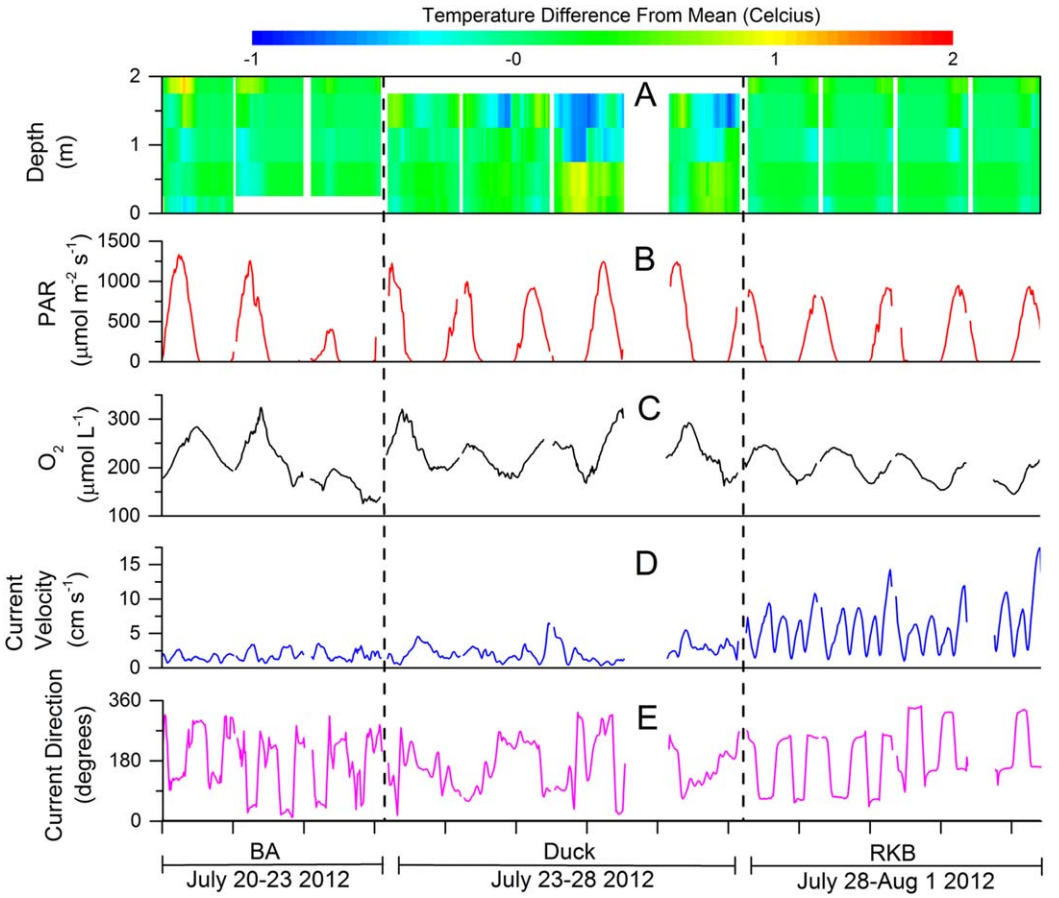

Figure 2. Time series (13 days) of typical conditions at all three sites. Vertical homogeneity was examined by plotting the change in temperature relative to the depth-averaged temperature across time (Figure 2a) where the white areas indicate no data. The average photosynthetically active radiation (PAR), O_2 concentration, depth-averaged current velocity, and current direction are shown in Figures 2b–2e, respectively. The depth-averaged current velocity was determined assuming a logarithmic velocity profile above the seagrass canopy. Periodic data gaps are due to the daily servicing of the instrumentation or changing between sites. The *x* axis indicates the site and dates of deployment at the site.

The daily integrated GPP and R rates from the Eulerian technique were not significantly different across the productivity gradient (Table 2, Figures 5 and 6). The NEM rates determined with the Eulerian technique were significantly different but did not show the expected trend across the nutrient gradient in Florida Bay (Figure 6 and Table 2). At Duck, the Eulerian GPP rates were significantly larger than the EC GPP rates and all of the Eulerian R rates were significantly higher than the EC R rates (at $p < 0.05$, Table 3).

The different components of the Eulerian flux (i.e., equation (1)) showed that the majority of the flux came from the local accumulation term ($\partial C/\partial t \cdot h$) at all sites (Figure 7). The horizontal advection component ($q_x \cdot \partial C/\partial x + q_y \cdot \partial C/\partial y$) had the second largest amplitude and decreased in magnitude with the decreasing velocity across the sites (Figure 7 and Table 1). The flux of O_2 across the water-air interface (Term 4, J_{gas}) was the smallest term but had the highest amplitude at BA, followed by Duck and RKB. The mean wind direction over the Eulerian deployments was 111 ± 47 ($\pm$ SD) degrees and the distance to land or shallow banks in this direction (indicating fetch for wave propagation) was approximately 1900, 650, and 3250 m for RKB, BA, and Duck, respectively.

3.2. Eddy Covariance

The site characteristic gradients were consistent with the observed EC rates measured across Florida Bay (Figure 3). The high efficiency of light utilization at RKB (largest seagrass biomass) is apparent from the photosynthesis—irradiance (P-I) relationships, where RKB had the steepest slope (0.81) and Duck (lowest seagrass biomass) had the smallest slope (0.16) (Figure 4). Differences in the slope of the linear P-I relationship

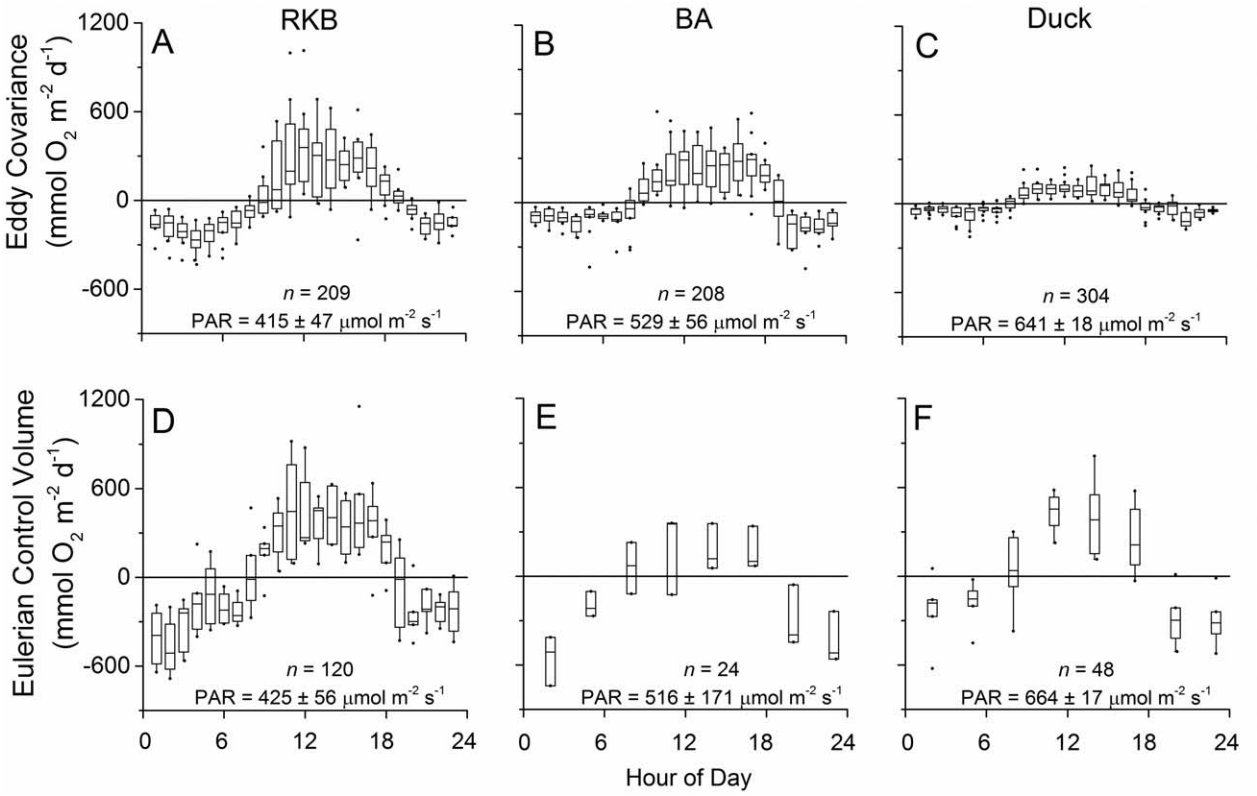

Figure 3. Hourly box plots of all eddy covariance (a, b, and c) and Eulerian control volume (d, e, and f) O_2 flux data for each site across the hour of day. The boxes represent the upper and lower quartile, the line in each box represents the median, the lines show the first outlier, and the circles represent outliers. The reduced data in Figures 3e and 3f were due to the low current velocities that reduce the response time of the Eulerian technique (flux rates at 3 h intervals for BA and Duck). The *n* is the number of individual flux estimates. PAR is the average photosynthetically active radiation over the time period of the measurements.

derived from the EC method were linearly proportional to differences in seagrass aboveground biomass per area ($r^2 = 1.00$, $p = 0.0011$, $n = 3$) [*Long et al*., 2015].

Integrating the EC fluxes over a 24 h period revealed rates of GPP and R that varied significantly across the sites (Table 2 and Figure 5). The highest rates of GPP, R, and NEM were at RKB and the lowest rates were at Duck, which were consistent with the predominant gradients in nutrients and seagrass biomass within in Florida Bay (Figures 5 and 6). The EC footprint, or the benthic surface that contributes to the flux, was estimated to be an ellipse upstream of the instrument of between 20 and 40 m long based on equations determined from tracer modeling by *Berg et al*. [2007]. The response time of the EC instrument, or the time it takes O_2 released at the benthic surface to reach the instrument was estimated to be < 5 min based on the modeling of tracer dispersion by *Rheuban and Berg* [2013].

The spectra of the vertical velocity indicated that both current flow-dominated conditions (Figure 8a) and wave-dominated conditions (Figure 8b) were present at different times, which were also consistent with the O_2 spectra (Figures 8c and 8d). All spectra showed a well-defined inertial subrange characterized by a $-5/3$ slope line. Wave dominated periods showed a distinct wave signal in the 0.5–1 Hz band, indicative of small surface waves. The cumulative cospectra in current flow dominated periods indicated flux contributions over a wider frequency band (0.002–0.9 Hz; Figure 8e) while wave dominated periods had an additional contribution to the flux at the wave frequencies (Figure 8f).

3.3. Biomass Addition

Measurements of biomass addition produced rates of aboveground seagrass production or NPP over the entire study period (weeks) that averaged the shorter-term (hourly) variations observed by the Eulerian and EC measurements. Thus, this method produced a single NPP value for each site that decreased from Duck to RKB with decreasing seagrass biomass and sediment nutrients (Table 2 and Figure 6). NPP rates derived

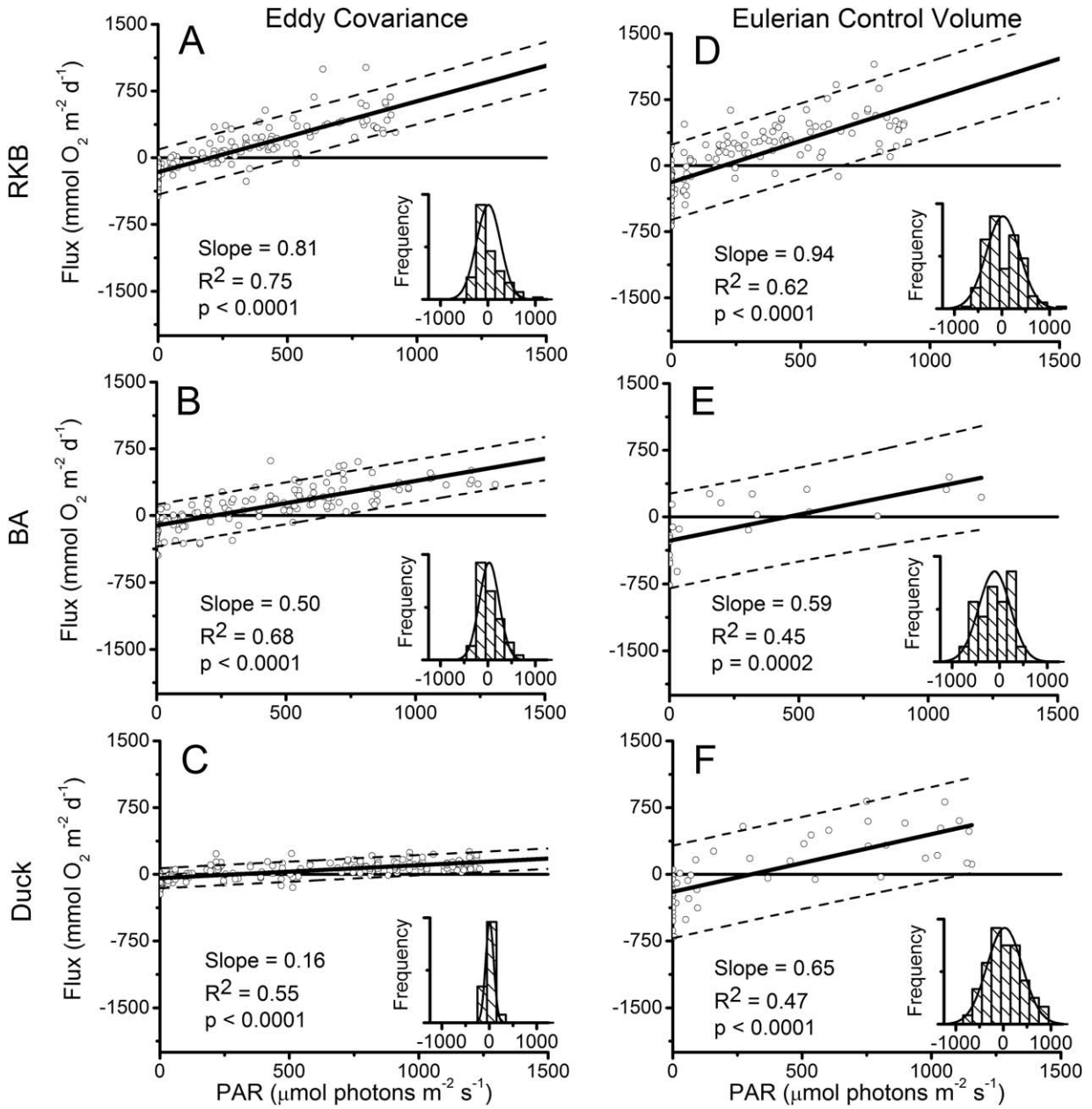

Figure 4. Linear regressions (solid lines) and 95% confidence intervals (dashed lines) for photosynthesis—irradiance relationships for each site by eddy covariance (a, b, and c) and Eulerian control volume methods (d, e, and f). The circles represent the response time of each technique at each site: 1 h for all eddy covariance measurements and the Eulerian technique at RKB, and 3 h for the Eulerian technique at BA and Duck. The inset figure in each plot is a histogram of the presented fluxes in 200 mmol O_2 m^{-2} d^{-1} bins.

from the marking technique were also more than double NEM rates derived from EC across all sites (2.0, 2.1, and 2.7 times greater for RKB, BA, and Duck, respectively).

4. Discussion

4.1. Spatial and Temporal Resolutions

The three methods examined (EC, Eulerian control volume, and the biomass addition) all operate at different spatial and temporal resolutions. The simplest and most-frequently used method was the biomass addition technique which determined a single estimate of seagrass NPP at long time scales (weeks) but at very small spatial scales (<0.1 m^2). In contrast, the EC technique determined benthic fluxes over both much

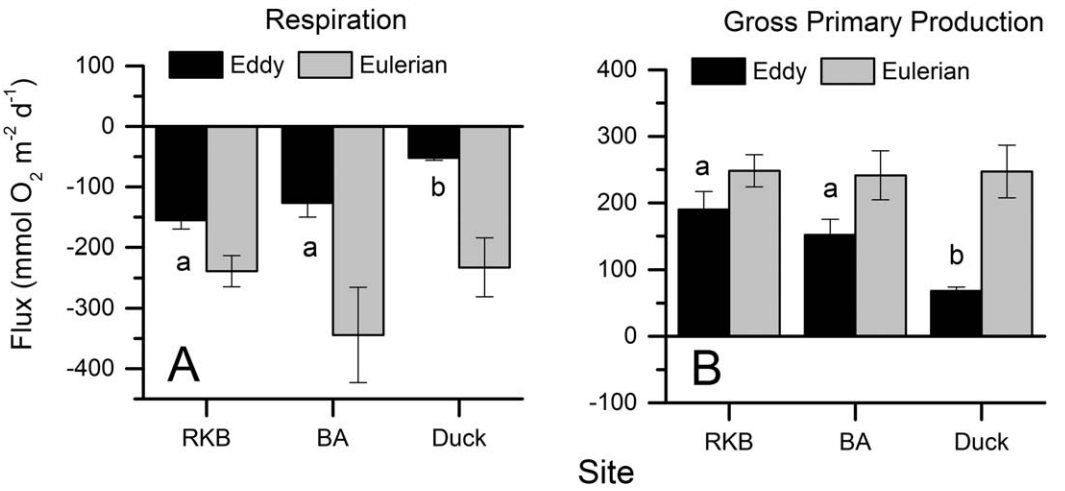

Figure 5. The left plot shows the respiration (R) rates across the sites by eddy covariance and Eulerian control volume methods (see Table 2 for statistics). The right plot shows the gross primary production (GPP) rates across the sites by eddy covariance and Eulerian methods. The lowercase letters above the bars represent significant differences ($p \leq 0.05$) across the sites for each method determined by ANOVA Tukey post tests where no letters indicate no differences. The error bars are standard errors.

shorter timescales (<1 h) and much larger spatial scales (10s of m^2) but was more technologically challenging. It not only required significant data processing and evaluation, but used sensors that frequently malfunction and foul, thereby limiting the deployment time. The Eulerian control volume technique averaged over an even larger spatial scale than EC (100s of m^2), but also resolved somewhat longer time scales (~hours). Given the existing rate of failure of the O_2 microelectrodes (44%), the control volume approach currently can be continuously deployed over much longer time periods (days to weeks) than the eddy covariance approach (~1 day). However, we expect that O_2 microelectrodes will continue to improve through ongoing technological development so that differences between the durability of O_2 microelectrodes and macrooptodes under real-world conditions will diminish over time.

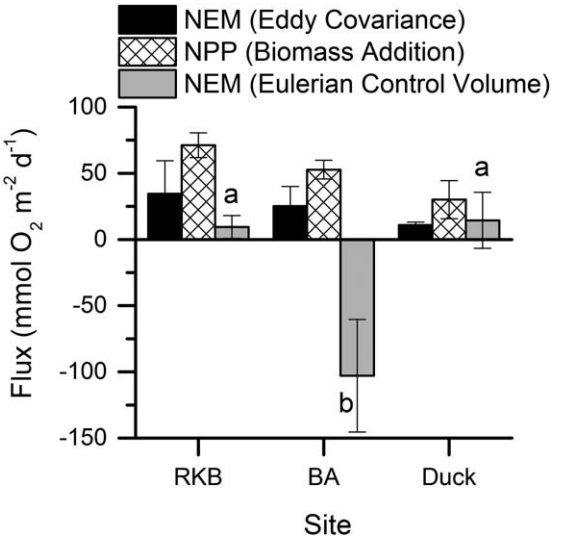

Figure 6. The net metabolism rates across the sites by eddy covariance, biomass addition, and Eulerian control volume methods. The eddy covariance and biomass addition techniques show the expected trend across the productivity gradient in Florida Bay. The > 2:1 ratio between the biomass addition and eddy technique is because the biomass addition technique only incorporates seagrass respiration and aboveground production whereas the eddy covariance technique incorporates all the organisms present in the seagrass meadow. The lowercase letters above the bars represent significant differences ($p \leq 0.05$) between sites for each method determined by ANOVA Tukey post tests where no letters indicate no differences. The error bars are standard errors.

The high temporal resolution of both the EC and Eulerian control volume techniques allows for the examination of how benthic metabolism responds to short-term variation in key environmental drivers such as light and flow [*Berg et al.*, 2003; *Hume et al.*, 2011; *Long et al.*, 2015]; however, there are tradeoffs between resolving versus averaging over this high-frequency variability. For example, the high-frequency EC rates can capture both large diel variations (average ± 300 mmol m^{-2} d^{-1}, Figure 3) as well as rapid responses to changes in environmental conditions (−500 to 1000 mmol m^{-2} d^{-1}, Figure 3); therefore, error estimates for daily benthic community metabolism derived from either EC or the Eulerian control volume fluxes will be affected by this naturally high variability (Table 2, Figures 5 and 6). In contrast, the biomass technique produces replicate NPP rates that integrate across weeks, with the error estimates primarily due to methodological artifacts (e.g., small areal coverage as well as

Table 3. Eddy Covariance Versus Eulerian Control Volume ANOVAs by Site

Site	Metabolism	F_1	p
RKB	R	7.9859	0.0153
	GPP	2.5891	0.1336
	NEM	0.8957	0.3626
BA	R	13.7475	0.0049
	GPP	4.0581	0.0748
	NEM	13.9439	0.0047
Duck	R	28.7213	<0.0001
	GPP	43.5628	<0.0001
	NEM	0.0525	0.8216

variation in shoot density, weight and % carbon content) that were unrelated to the diel variability observed with the EC and Eulerian methods.

The fast-response metabolic rates from EC (benthic) and Eulerian (benthic + water column) techniques are compared here, despite the fact that they integrate over different ecosystem components. This comparison can be made because the water column metabolic rates did not vary significantly across the productivity gradient and were on average an order of magnitude lower than the Eulerian and EC metabolic rates (Table 2); similar to other oligotrophic, benthic dominated systems such as coral reefs [*Kinsey*, 1985]. These low water column metabolism rates are due to the clear, nutrient-depleted waters of Florida Bay that result from long water residence times and low nutrient inputs [*Fourqurean and Zieman*, 1992, 2002].

4.2. Eulerian Control Volume

For the Eulerian control volume, the local accumulation term ($\partial C/\partial t \cdot h$) was the largest contributor to the flux at all sites and was of similar magnitude to the amplitude of the total net flux (90–99%, Figure 7). This is in contrast to prior measurements made in higher flow systems were the advective terms are dominant [*Falter et al*., 2008, 2012]. The amplitude of the advective or horizontal flux ($q_x \cdot \partial C/\partial x + q_y \cdot \partial C/\partial y$) varied from 35 to 88% of the amplitude of the total net flux and scaled with the average velocities at each site (Table 1). Therefore, the inclusion of horizontal transport and multiple point measurements in the Eulerian control volume approach has significant advantages over single-point open water methods that rely on measurements made only at one location [e.g., *Odum*, 1957, *Kinsey*, 1978]; even for the relatively sluggish flow regimes here.

Estimating the flux of O_2 across the water-air interface (J_{gas}) can be challenging due to the difficulty of relating actual gas exchange rates to near-surface wind-stress, turbulence, and/or roughness [*Zappa et al*., 2003; *Ho et al*., 2006; *Falter et al*., 2008]. The variability of the water surface due to wind velocities was likely impacted by the shallow banks and islands throughout Florida Bay and likely resulted in errors in estimating J_{gas}. The RKB, BA, and Duck sites were located 1900, 650, and 3250 m away, respectively, from the nearest emergent features in the dominant wind direction. While RKB and Duck had a significant distance for wave propagation, it is likely that the reduced fetch at BA led to an overestimate of the transfer of O_2 across the air-water interface compared to RKB and Duck that resulted in an overestimate of respiration at BA. This likely contributed to the large negative NEM for BA (Figure 6) which was inconsistent with the EC and biomass metabolism rates as well as historical data from this site [*Fourqurean and Zieman*, 1992, 2002]. Current velocities have also been shown to cause enhanced gas exchange [*Zappa et al*., 2003] but the low velocities observed here (Table 1) and the agreement between the methods at the highest velocity site of RKB indicate that this effect was likely negligible.

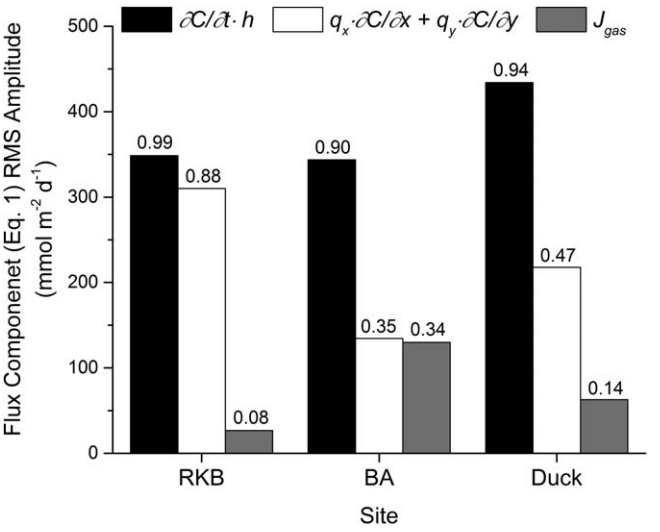

Figure 7. The RMS amplitude of the individual components of the Eulerian fluxes by site from the differential form of the advection-dispersion-reaction (equation (1)). Numbers above bars represent the ratio of the RMS amplitude of each flux component to the RMS amplitude of the net oxygen flux (352, 383, and 462 mmol m^{-2} d^{-1}, for RKB, BA, and Duck, respectively).

The significantly larger R and GPP rates (Table 3 and Figure 4) by the

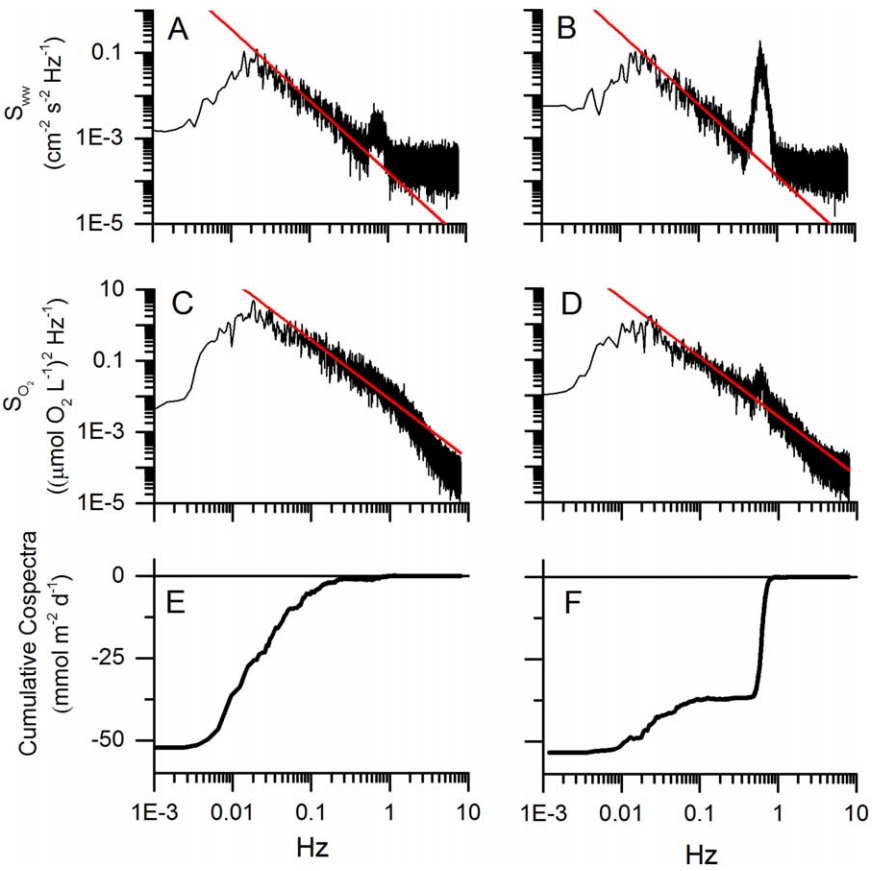

Figure 8. Eddy covariance measurements dominated by current flow (left) and wave action (right). The vertical velocity spectra (a, b) and oxygen spectra (c, d) showed inertial subrange regions indicated by the red line with a −5/3 slope. Each spectrum is from 1.5 h of data on the same night at the Duck Key site. Cumulative cospectra showed that the same size fluxes were obtained under both current flow-dominated and wave-dominated conditions (e versus f, respectively). Mean current flow velocity was 1.7 ± 0.6 and 1.0 ± 0.1 cm s^{-1} for current flow-dominated and wave-dominated conditions, respectively. Associated significant wave heights were 0.9 ± 0.1 and 3.3 ± 0.3 cm, respectively.

Eulerian technique could not be explained by increasing the transfer of O_2 across the water-air interface, as J_{gas} was a small component of the flux at both RKB and Duck (Figure 6). However, the NEM rates are small in comparison to the GPP and R rates and could be significantly influenced by the J_{gas} rates, leading to errors in the net metabolic status of ecosystems (i.e., Figure 6). For example, when the gas exchange coefficient (k_{O_2}) was doubled [e.g., *Falter et al*., 2008], variations in the daily Eulerian NEM rates of −12 to 67 mmol m^{-2} d^{-1} were found (data not shown), which is on the same order as the net metabolic rates determined by all three methods. Thus, uncertainties in the gas flux can substantially affect estimates of daily net fluxes (NEM) in communities where the pathways of carbon fixation and consumption are evenly matched (P ∼ R). These include the present seagrass communities as well as reef communities in general [*Kinsey*, 1985]. In contrast, estimates of net daily fluxes derived from EC measurements are not subject to the same errors in gas fluxes since they measure convective mass fluxes close to the benthos and away from the air-sea interface.

The Eulerian control volume data were also potentially influenced by the control volume size, the O_2 optode accuracy, and stratification in the water column. A trade-off exists between the control volume size and the sensor resolution and accuracy, where a larger control volume needs more time for water to travel across it but requires less sensor resolution [*Genin et al*., 2009; *Teneva et al*., 2013]. The size of the present control volume was chosen to ensure large differences were observed by the O_2 optodes. The manufacturer reported accuracy is ± 5% or roughly ±10 μmol L^{-1} given the oxygen concentrations measured here (150–300 μmol L^{-1}); however, we were able to calibrate the optodes to a much greater accuracy on our own (±3 μmol L^{-1}) by correcting for sensor drift and salinity. We tested the sensitivity of the Eulerian technique to the optode accuracy by changing the observed O_2 concentrations at one of the control volume apices at BA by −10 and +10 μmol L^{-1}. Despite this 20 μmol L^{-1} error range, no significant changes in the R, GPP, or NEM

rates were observed (ANOVAs; $F = 0.07$, $p > 0.94$) and only resulted in maximum changes of +6 to −9 mmol m^{-2} d^{-1} in the NEM rates, which could not explain the large differences between the methods at BA. However, we recognize that the accuracy of the O_2 sensors can be more of an issue in more advectively dominated habitats [*Falter et al*., 2008]. The length of time it took a water parcel to move across the control volume, especially during low-current periods, and the changing of the current direction (e.g., Figure 2) also likely increased the variability of the Eulerian fluxes. Further, while most periods showed a well-mixed water column (Figure 2a), Eulerian variability may have been increased by periodic stratification, especially at the low-velocity sites of Duck and BA. This stratification may have inhibited the necessary vertical mixing such that O_2 measurements taken at a specific height in the water column could not properly represent depth-averaged concentrations; a condition necessary for simplifying the resulting time-dependent mass balance into two rather than three dimensions. The presence of stratification would have further caused error in determining the depth-integrated current or transport from our single-point velocity measurements; however, this was probably not as important an issue for the present field sites given that the advective component of the total nonconservative reactive transport was generally smaller than the local time-dependent components. Unfortunately, we did not have vertical O_2 gradients and lacked temperature gradient data for all periods, and therefore could not use it to remove stratified periods from the Eulerian data or evaluate the assumptions about the vertical water column structure.

4.3. Eddy Covariance

Stratification generally only affects EC measurements when it limits flow near the sediment boundary and reduces turbulence [*Brand et al*., 2008; *Long et al*., 2012a] and was generally not observed near the sediment surface in the temperature profiles (Figure 2a). Temporal changes in vertical O_2 gradients due to horizontal transport of water masses with different O_2 concentrations can also intermittently distort the EC flux estimates [*Holtappels et al*., 2013]. However, when integrated over longer periods of time (e.g., to calculate R, GPP, NEM), the effects of these short-lived biases are minimal [*Holtappels et al*., 2013]. This greater resilience of EC measurements to the vertical structure in the water column suggests that EC should provide a more robust approach to measuring benthic net production than Eulerian control volumes in systems such as Florida Bay that are subject to weak currents, rapidly changing current directions, or limited stratification due to natural variability in temperature or salinity.

The accuracy of the EC flux rates may also be influenced by the orientation of the EC velocimeter, the storage of O_2 in the water column, and sensor malfunction. The orientation of the velocimeter is important because a sensor tilt can bias the small-magnitude vertical velocity through the inclusion of some of the larger-magnitude horizontal velocity components. This bias was investigated through a two-step rotation of the velocity coordinates [*Berg et al*., 2003] and was found to have no significant effect on the flux [*Long et al*., 2015]. The storage of O_2 in the water column, or the loss of some of the flux signal to changing the water column O_2 concentration, was a source of bias in the EC flux rates measured at height above the benthic surface. The correction for this storage [see *Rheuban et al*., 2014] was found to significantly affect the fluxes and was therefore included in the flux estimates [*Long et al*., 2015]. In general, the storage correction increased the magnitude of the measured EC fluxes and therefore could not explain the larger Eulerian flux estimates, unless the storage correction was underestimated. Further, this storage correction was also sensitive to short-term O_2 changes in the water column and therefore led to increased error in the determined hourly flux rates, but likely did not affect the long-term (daily to weekly) estimates as these short-term variations average out across diel scales [*Holtappels et al*., 2013]. Sensor malfunction and fouling led to a significant loss of EC data, as determined by comparison to the stable macro O_2 sensors, but short-term disruption and fouling of the high-frequency O_2 microsensors may have also occurred, but are currently difficult to evaluate. Future applications of EC would benefit from video cameras to determine when this sensor disruption occurs and the development of sensors that are resistant to fouling.

The orbital water motion produced by passing surface gravity waves can greatly affect the vertical convection of mass and momentum in shallow water benthic communities [*Koch and Gust*, 1999; *Reidenbach et al*., 2007; *Hansen and Reidenbach*, 2012; *Lowe and Falter*, 2015]. Our measured wave heights (∼3 cm) were small but nonetheless produced vertical orbital velocities that were similar in scale to the mean current velocities (± 1 cm s^{-1} versus 2–5 cm s^{-1}), which were evident in the vertical velocity spectra (e.g., Figures 8a and 8b). Unlike current-driven turbulent eddy motions, wave orbital motions are irrotational, yet they can still contribute to the total vertical mass transport through the covariance between the vertical wave orbital

velocities and the variance in the O_2 concentration (Figure 8f) [*Kuwae et al*., 2006; *Chipman et al*., 2012; *Reimers et al*., 2012]; due to either the advection of the turbulent motions or the O_2 variances themselves [*Lumley and Terray*, 1983; *Gerbi et al*., 2009]. The height of our measurements (35–55 cm above the bottom) were made well outside any wave boundary layer (~1 cm) [*Sleath*, 1987; *Nielsen*, 1992], so it is unlikely there was any substantial influence of wave-generated turbulence on our measurements of vertical transport. However, our fixed-point measurements may also be influenced by an apparent wave-bias where the vertical velocities can be biased by horizontal orbital motions due to uncertain velocimeter orientation [*Trowbridge*, 1998; *Reimers et al*., 2012]. The presented data were not sensitive to a two-step rotation of the velocity field into the main current direction, even during low-flow and high-wave periods, suggesting that any apparent wave-bias was insignificant.

The extent to which the net vertical transport of O_2 is due to wave-driven advection of water column turbulence, advection of vertical gradients in bulk water O_2 concentration, or simply eddy transport at wave-like frequencies is not currently well-described. While a proper decomposition of the exact physical mechanisms responsible for vertical mass transport should be the subject of future studies, our measurements nonetheless capture most if not all of the net vertical advection of water column O_2 concentrations through a natural covariance between the mass and velocity spectra, regardless of the physical mechanisms responsible. In this sense, the term "eddy covariance" is simply a convenient terminology borrowed from the atmospheric boundary layer literature to describe a more universal method capable of integrating multiple mechanisms of net vertical mass transport. The most compelling evidence that our measurements were properly measuring net rates of metabolism by seagrass communities, independent of the modest background wave activity, is (1) the lack of any correlation between variations in significant wave height and both the daytime and nighttime fluxes, (2) that similar rates of nighttime respiration were found under both wave-dominated and current-dominated periods (Figure 8), and (3) that the net fluxes averaged over a 24 h period as measured by the EC method closely match the trends in the long-term rates of net primary production by the dominant seagrass (Figure 6).

4.4. Comparison Across Florida Bay

The EC flux measurements were consistent with the established productivity and nutrient gradient across Florida Bay [*Zieman*, 1989; *Fourqurean and Zieman*, 1992; *Long et al*., 2008] with the highest average and instantaneous rates at Rabbit Key Basin (RKB) and the lowest at Duck Key (Duck) (Figures 3 and 5). In contrast, the Eulerian control volume measurements did not show any trends or significant differences across the nutrient and productivity gradient (Figure 5). This lack of variability across the well-established productivity and nutrient gradient is likely due to uncertainties associated with the Eulerian technique used under the present conditions [*Atkinson and Grigg*, 1984; *Ziegler and Benner*, 1998; *Falter et al*., 2008; *McGillis et al*., 2011]; particularly given that it is a low-energy environment subject to episodic stratification and changes in current direction. The greatest agreement between the Eulerian control volume and EC was found at site RKB (Figures 3a and 3d), likely due to the higher rates of benthic metabolism as well as conditions of higher flow and a more vigorously mixed water column (Table 1). However, results from both methods became increasingly different across the decreasing productivity gradient as the prevailing currents got weaker and stratification became more prominent (Figures 3 and 4). The high variance and broader frequency distributions of the Eulerian technique were most obvious at the isolated site Duck (Figure 4f) where the 95% confidence intervals for the Eulerian P-I relationship were much larger despite this site having the most data from both techniques (6 and 12 days for the Eulerian and EC methods, respectively). *Falter et al*. [2012] found much higher correlations between incident light and hourly rates of production in a coral-dominated reef flat community in northwest Australia; however, that was under advectively dominated and vertically well-mixed flow conditions where the rates of daily benthic production were 4–5 times higher than the seagrass communities studied here (GPP = 1000 to 1500 mmol C m^{-2} d^{-1}). The Eulerian method also produced average R rates that were significantly larger than those determined by EC at all sites (Table 3). The Eulerian R rates were on average 160 mmol m^{-2} d^{-1} larger than EC rates and cannot be explained by water column metabolism rates (Table 2). Stratification in the water column may have led to higher estimates of R due to the height of the water column affected by benthic processes being effectively reduced and the overestimate of the depth-integrated current velocity. The larger magnitude metabolism rates of the Eulerian technique, especially in these shallow, low-flow environments warrants further investigation as it has large implications for the net carbon cycling and storage in shallow, highly productive seagrass ecosystems.

Although no differences in R and GPP rates were observed across the sites with the Eulerian technique, it is important to note that long time series of Eulerian data are needed to accurately determine the metabolism of ecosystems [*Falter et al*., 2008; *McGillis et al*., 2011]. The reduced amount of data presented here (3–12 diel cycles) likely contributed to the differences between the methods as periods of up to 12 days for EC data were found to introduce variability for seasonal metabolism estimates [*Long et al*., 2015]. Due to the much higher variance in the Eulerian data, we expect the period of integration to be significantly longer than 12 days for Eulerian estimates of seasonal metabolism at similar sites. Future studies using the EC and Eulerian techniques should focus on instrumentation that is able to sample over longer time periods to provide accurate estimates of ecosystem metabolism.

4.5. Seagrass Meadow Metabolism

The difference in the productivity of seagrasses across Florida Bay is largely due to a gradient in phosphorus limitation [*Fourqurean and Zieman*, 1992, 2002; *Long et al*., 2008] and our results are consistent with this assertion (Tables 1 and 2). This nutrient-driven productivity gradient was observed in the different slopes of the P-I relationships across the sites that were directly related to the amount of seagrass biomass [*Long et al*., 2015]. The vertical structure of seagrass canopy creates a large photosynthetic surface area while spreading out the incoming irradiance over a large area [*Binzer et al*., 2006; *Sand-Jensen et al*., 2007]. This canopy structure increases the light-capturing efficiency of the seagrass ecosystem resulting in linear P-I relationships [*Rheuban et al*., 2014; *Long et al*., 2015] as seen in both the Eulerian and EC data (Figure 4).

The contributions of different communities to the total seagrass ecosystem metabolism can be examined based on the differences between the methods used in this study. The biomass technique measured the net primary production (NPP) of the aboveground seagrass biomass [*Zieman*, 1974] which included the respiration of the above and belowground biomass but did not include belowground growth [*Kemp et al*., 1990]. Therefore, the seagrass NPP rates represent conservative estimates of the total productivity by seagrasses. Further, the marking technique only measures the net primary production of seagrass and does not incorporate benthic microalgae, macroalgae, sediment respiration, epiphytes, or other heterotrophs in the seagrass ecosystem. The more than twofold higher marking NPP rates across all sites in Florida Bay compared with EC rates of NEM (Figure 6) indicate that the combination of other producers, consumers, and belowground seagrass growth was net heterotrophic in seagrass meadows and that these groups are also likely limited in growth by the nutrient gradient and/or biomass gradient across the bay. This heterotrophic component of seagrass meadows is very important to the carbon budgets of seagrasses given they can store as much as two thirds of their carbon in belowground biomass and organic rich soils [*Duarte et al*., 2010; *Fourqurean et al*., 2012]. Therefore, the net carbon that is stored belowground in seagrass meadows is highly dependent upon the net respiration by these heterotrophic communities.

A simple, first-order estimation of the total carbon exchange determined from each method exhibits the importance of determining accurate metabolic rates while acknowledging the limitations of each method. For example, the total coverage of seagrass habitat within Florida Bay is estimated to be 145,300 Ha [*Yarbro and Carlson*, 2013]. Assuming that the average NEM of the EC measurements across the nutrient gradient accurately represent the average net flux of fixed carbon across Florida Bay (24 mmol C m^{-2} d^{-1}), the average net storage of fixed carbon in the seagrass meadows of Florida Bay was about 410 mT C d^{-1} over the study period. Using the rate from the biomass addition technique (900 mT d^{-1}) and the differences between the methods, it was determined that the net effect of all other organisms (excluding seagrasses) plus belowground growth was to decrease the net carbon exchange of seagrass meadows by $\sim$ 50%. Last, the net fluxes of fixed carbon as estimated from the Eulerian measurements were either negative (BA) or not significantly different from zero (Duck and RKB). Either way, results from the Eulerian measurements contrast with those from the biomass addition and EC measurements and also contradict the prevailing view that seagrass meadows are net sinks of fixed carbon [*Duarte et al*., 2010; *Fourqurean et al*., 2012].

5. Conclusions

While EC and Eulerian control volume approaches may both be well suited for measuring diurnal changes in net benthic O_2 fluxes and daily rates of gross metabolism, the EC approach is likely better-suited for estimating net O_2 fluxes integrated over a full diel cycle. Furthermore, the EC approach is likely better-suited for making short-term measurements of net O_2 fluxes in low-energy coastal habitats due to it being less

sensitive to the kind of episodic stratification commonly found in these environments. The Eulerian control volume method still has some significant advantages over the EC technique including the ability to sample over larger spatial and longer temporal scales as well as being applicable to nearly any solute that can be measured within minutes to hours (compared to less than a second required for EC). Both the EC and Eulerian methods would benefit from new sensors that are specifically designed to have the high accuracy, high resolution, and fast response time required for these in situ methods as well as being more resilient to damage and biofouling. Finally, a careful evaluation of the water column structure in low-flow coastal systems would significantly enhance the ability to evaluate future measurements of net production derived from either EC or Eulerian control volume data.

Acknowledgments

This manuscript is dedicated to the memory of Joseph C. Zieman, the pioneer of the seagrass "biomass addition technique" and a great friend and mentor. Data for this paper can be accessed at https://knb.ecoinformatics.org. This research was conducted under Everglades National Park permit # EVER-2011-SCI-0057. This study received financial support from the Jones Environmental and Barley Scholars Program at the University of Virginia and the National Science Foundation (Chemical Oceanography grant OCE-0536431). We thank Alexandra Van Horn and Susan Gordon for assistance in the field.

References

Atkinson, M. J., and R. W. Grigg (1984), Model of a coral reef ecosystem. Part II: Gross and net benthic primary production at French Frigate Shoals, Hawaii, *Coral Reefs*, *3*, 13–22.

Baldocchi, D. (2003), Assessing the eddy covariance technique for evaluating carbon dioxide exchange rates of ecosystems: Past, present and future, *Global Change Biol.*, *9*, 479–492.

Berg, P., H. Roy, F. Janssen, V. Meyer, B. B. Jorgensen, M. Huettel, and D. De Beer (2003), Oxygen uptake by aquatic sediments measured with a novel non-invasive eddy correlation technique, *Mar. Ecol. Prog. Ser.*, *261*, 75–83.

Berg, P., H. Roy, and P. L. Wiberg (2007), Eddy correlation flux measurements: The sediment surface area that contributes to the flux, *Limnol. Oceanogr.*, *52*, 1672–1684.

Berg, P., R. Glud, A. Hume, H. Stahl, K. Oguri, V. Meyer, and H. Kitazato (2009), Eddy correlation measurements of oxygen uptake in deep ocean sediments, *Limnol. Oceanogr. Methods*, *7*, 576–584.

Berg, P., M. H. Long, M. Huettel, K. McGlathery, J. Rheuban, A. Giblin, R. Howarth, R. Marino, and K. Foreman (2013), Eddy correlation measurements of oxygen fluxes for permeable sediments exposed to varying current flows, *Limnol. Oceanogr.*, *58*, 1329–1343.

Binzer, T., K. Sand-Jensen, and A. L. Middleboe (2006), Community photosynthesis of aquatic macrophytes, *Limnol. Oceanogr.*, *51*, 2722–2733.

Brand, A., D. F. McGinnis, B. Wehrli, and A. Wuest (2008), Intermittent oxygen flux from the interior into the bottom boundary of lakes as observed by eddy correlation, *Limnol. Oceanogr.*, *53*, 1997–2006.

Broecker, W. S., and T. H. Peng (1982), *Tracers in the Sea*, 690 pp., Eldigio, N. Y.

Burba, G. (2013), *Eddy Covariance Method*, Li-COR Biogeosci., 329 pp., Lincoln, Nebraska.

Chipman, L., M. Huettel, P. Berg, V. Meyer, I. Klimant, R. Glud, and F. Wenzhoefer (2012), Oxygen optodes as fast sensors for eddy correlation measurements in aquatic systems, *Limnol. Oceanogr. Methods*, *10*, 304–316.

Cole, J. J., M. L. Pace, S. R. Carpenter, and J. F. Kitchell (2000), Persistence of net heterotrophy in lakes during nutrient addition and food web manipulations, *Limnol. Oceanogr.*, *45*, 1718–1730.

Dean, R. G., and R. S. Dalrymple (1991), *Water Wave Mechanics for Engineers and Scientists*, 2nd ed., 353 pp., World Sci.

Duarte, C. M., and C. L. Chiscano (1999), Seagrass biomass and production: A reassessment, *Aquat. Bot.*, *65*, 159–174.

Duarte, C. M., N. Marba, E. Gacia, J. W. Fourqurean, J. Beggins, C. Barron, and E. T. Apostolake (2010), Seagrass community metabolism: Assessing the carbon sink capacity of seagrass meadows, *Global Biogeochem. Cycles*, *24*, GB4032, doi:10.1029/2010GB003793.

Falter, J. L., R. J. Lowe, M. J. Atkinson, S. G. Monismith, and D. W. Schar (2008), Continuous measurements of net production over a shallow reef community using a modified Eulerian approach, *J. Geophys. Res.*, *113*, C07035, doi:10.1029/2007JC004663.

Falter, J. L., R. J. Lowe, M. J. Atkinson, and P. Cuet (2012), Seasonal coupling and de-coupling of net calcification rates from coral reef metabolism and carbonate chemistry at Ningaloo Reef, Western Australia, *J. Geophys. Res.*, *117*, C05003, doi:10.1029/2011JC007268.

Fourqurean, J. W., and J. C. Zieman (1992), Phosphorus limitation of primary production in Florida Bay: Evidence from C:N:P ratios of the dominant seagrass Thalassia testudinum, *Limnol. Oceanogr.*, *37*, 162–171.

Fourqurean, J. W., and J. C. Zieman (2002), Nutrient content of the seagrass Thalassia testudinum reveals regional patterns of relative availability of nitrogen and phosphorus in the Florida Keys, USA, *Biogeochemistry*, *61*, 229–245.

Fourqurean, J. W., et al. (2012) Seagrass ecosystems as a globally significant carbon stock, *Nat. Geosci.*, *5*, 505–509, doi:10.1038/NGEO1477.

Genin, A., S. G. Monismith, M. A. Reidenbach, G. Yahel, and J. R. Koseff (2009), Intense grazing of phytoplankton in a coral reef, *Limnol. Oceanogr.*, *54*, 938–951.

Gerbi, G. P., J. H. Trowbridge, E. A. Terray, A. J. Plueddemann, and T Kukulka (2009), Observations of turbulence in the ocean surface boundary layer: Energetics and diffusivity, *J. Phys. Oceanogr.*, *39*, 1077–1096.

Hansen, J. C. R., and M. A. Reidenbach (2012), Wave and tidally driven flows in eelgrass beds and their effect on sediment suspension, *Mar. Ecol. Prog. Ser.*, *448*, 271–287.

Ho, D. T., C. S. Law, M. J. Smith, P. Schlosser, M. Harvey, and P. Hill (2006), Measurements of air-sea gas exchange at high wind speeds in the Southern Ocean: Implications for global parameterizations, *Geophys. Res. Lett.*, *33*, L16611, doi:10.1029/2006GL026817.

Holtappels, M., R. N. Glud, D. Donis, B. Liu, A. Hume, F. Wenzhofer, and M. M. Kuypers (2013), Effects of transient bottom water currents and oxygen concentrations on benthic exchange rates as assessed by eddy correlation measurements, *J. Geophys. Res. Oceans*, *118*, 1157–1169, doi:10.1002/jgrc.20112.

Hume, A. C., P. Berg, and K. J. McGlathery (2011), Dissolved oxygen fluxes and ecosystem metabolism in an eelgrass (Zoster marina) meadow measured with the eddy correlation technique, *Limnol. Oceanogr.*, *56*, 86–96.

Kemp, M., L. Murray, and C. P. McRoy (1990), Primary productivity, in *Seagrass Research Methods, Monogr. Ocean Methodol. 8*, edited by R. C. Philips and C. P. McRoy, pp. 153–160, Unesco, Paris.

Kinsey, D. (1978), Productivity and calcification estimates using slack-water periods and field enclosures, in *Coral Reefs: Research Methods*, 281 pp., United Nations, Paris.

Kinsey, D. (1985), Metabolism, calcification and carbon production. I. System level studies. Proceedings of 5th International Coral Reef Symposium, *4*, 505–526.

Koch, E. W., and G. Gust (1999), Water flow in tide- and wave-dominated beds of the seagrass *Thalassia testudinum*, *Mar. Ecol. Prog. Ser.*, *184*, 63–72.

Koroleff, L. (1983), Determination of phosphorus, in *Methods of Seawater Analysis*, 125–131, Springer.

Kuwae, T., K. Kamio, T. Inoue, E. Miyoshi, and Y. Uchiyama (2006), Oxygen exchange flux between sediment and water in an intertidal sandflat, measured *in-situ* by the eddy-correlation method, *Mar. Ecol. Prog. Ser.*, *307*, 59–68.
Long, M. H., K. J. McGlathery, J. C. Zieman, and P. Berg (2008), The role of organic acid exudates in liberating phosphorus from seagrass-vegetated carbonate sediments, *Limnol. Oceanogr.*, *53*, 2616–2626.
Long, M. H., P. Berg, D. Koopmans, S. Rysgaard, and R. Glud (2012a), Oxygen metabolism and ice melt measured at the water-ice interface by eddy correlation, *Biogeosciences*, *9*, 1957–1967.
Long, M. H., J. Rheuban, P. Berg, and J. C. Zieman (2012b), A comparison and correction of versatile and economical light loggers to photosynthetically active radiation sensors, *Limnol. Oceanogr. Methods*, *10*, 416–424.
Long, M. H., P. Berg, D. De Beer, and J. Zieman (2013), In situ coral reef oxygen metabolism: An eddy correlation study, *PLoS One*, *8*, e58581.
Long, M. H., P. Berg, K. J. McGlathery, and J. C. Zieman (2015), Subtropical seagrass ecosystem metabolism measured by eddy correlation, *Mar. Ecol. Prog. Ser.*, doi:10.3354/meps11314, in press.
Lorke, A., D. F. Mcginnis, and A. Maeck (2013), Eddy-correlation measurements of benthic fluxes under complex flow conditions: Effects of coordinate transformations and averaging timescales, *Limnol. Oceanogr. Methods*, *11*, 425–437.
Lowe, R. J., and J. L. Falter (2015), Oceanic Forcing of Coral Reefs, *Ann. Rev. Mar. Sci.*, *7*, 43–66.
Lumley, J. L., and E. A. Terray (1983), Turbulence convected by a random wave field, *J. Phys. Oceanogr.*, *13*, 2000–2007.
Mass, T., A. Genin, U. Shavit, M. Grinstein, and D. Tchernov (2010), Flow enhances photosynthesis in marine benthic autotrophs by increasing the efflux of oxygen from the organism to the water, *Proc. Natl. Acad. Sci. U. S. A.*, *107*, 2527–2531.
McGillis, W. R., C. Langdom, B. Loose, K. K. Yates, and J. Corredor (2011), Productivity of a coral reef using boundary layer and enclosure methods, *Geophys. Res. Lett.*, *38*, L03611, doi:10.1029/2010GL046179.
McGinnis, D. F., S. Cherednichenko, S. Sommer, P. Berg, L. Rovelli, R. Schwarz, R. N. Glud, and P. Linke (2011), Simple, robust eddy correlation amplifier for aquatic dissolved oxygen and hydrogen sulfide measurements, *Limnol. Oceanogr. Methods*, *9*, 340–347.
Monismith, S. G., and D. A. Fong (2004), A note on the potential transport of scalars and organisms by surface waves, *Limnol. Oceanogr.*, *49*, 1214–1217.
Monismith, S. D, et al. (2010), Flow effects on benthic grazing on phytoplankton by a Caribbean reef, *Limnol. Oceanogr.*, *55*, 1881–1892.
Nielsen, P. (1992), *Coastal Bottom Boundary Layers and Sediment Transport*, vol. 4, 324 pp., World Sci.
Nepf, H. M. (2012), Flow and transport in regions with aquatic vegetation, *Annu. Rev. Fluid Mech.*, *44*, 123–142.
Odum, H. T. (1957), Primary production measurements in eleven Florida springs and a marine turtle-grass community, *Limnol. Oceanogr.*, *2*, 85–97.
Raymond, P. A., and J. J. Cole (2001), Gas exchange in rivers and estuaries: Choosing a gas transfer velocity, *Estuaries*, *24*, 312–317.
Reidenbach, M. A., J. R. Koseff, and S. G. Monismith (2007), Laboratory experiments of fine-scale mixing and mass transport within a coral canopy, *Phys. Fluids*, *19*, 075107.
Reimers, C. E., H. T. Özkan-Haller, P. Berg, A. Devol, K. McCann-Grosvenor, and R. D. Sanders (2012), Benthic oxygen consumption rates during hypoxic conditions on the Oregon continental shelf: Evaluation of the eddy correlation method, *J. Geophys. Res.*, *117*, C02021, doi:10.1029/2011JC007564.
Revsbech, N. P. (1989), An oxygen microsensor with a guard cathode, *Limnol. Oceanogr.*, *34*, 474–478.
Rheuban, J. E., and P. Berg (2013), The effects of spatial and temporal variability at the sediment surface on aquatic eddy correlation flux measurements, *Limnol. Oceanogr. Methods*, *11*, 351–359.
Rheuban, J. E., P. Berg, and K. J. McGlathery (2014), Multiple timescale processes drive ecosystem metabolism in eelgrass (*Zostera marina L.*) meadows, *Mar. Ecol. Prog. Ser.*, *507*, 1–13, doi:10.3354/meps10843.
Sand-Jensen, K., T. Binzer, and A. L. Middleboe (2007), Scaling of photosynthetic production of aquatic macrophytes: A review, *Oikos*, *116*, 280–294.
Sleath, J. F. (1987), Turbulent oscillatory flow over rough beds, *J. Fluid Mech.*, *182*, 369–409.
Teneva, L., R. B. Dunbar, D. A. Mucciarone, J. F. Dunckley, and J. R. Koseff (2013), High-resolution carbon budgets on a Palau back-reef modulated by interactions between hydrodynamics and reef metabolism, *Limnol. Oceanogr.*, *58*, 1851–1870.
Thomas, F. I. M., and C. D. Cornelisen (2003), Ammonium uptake by seagrass communities: Effects of oscillatory versus unidirectional flow, *Mar. Ecol. Prog. Ser.*, *247*, 51–57.
Trowbridge, J. H. (1998), On a technique for measurement of turbulent shear stress in the presence of surface waves, *J. Atmos. Oceanic Technol.*, *15*, 290–298.
Wiberg, P. L., and C. R. Sherwood (2008), Calculating wave-generated bottom orbital velocities from surface-wave parameters, *Comput. Geosci.*, *34*, 1243–1262.
Yarbro, L. A., and P. R. Carlson (Eds.) (2013), Seagrass integrated mapping and monitoring program: Mapping and monitoring report number 1, *Tech. Rep. TR-17*, 126 p., Fish and Wildlife Res. Inst., Fla.
Zappa, C. J., P. A. Raymond, E. A. Terray, and W. R. McGillis (2003), Variation in surface turbulence and the gas transfer velocity over a tidal cycle in a macro estuary, *Estuaries*, *26*, 1401–1415.
Ziegler, S., and R. Benner (1998), Ecosystem metabolism in a subtropical, seagrass-dominated lagoon, *Mar. Ecol. Prog. Ser.*, *173*, 1–12.
Zieman, J. C. (1974), Methods for the study of the growth and production of the turtle grass, *Thalassia testudinum, Aquaculture*, *4*, 139–143.
Zieman, J. C. (1989) Distribution, abundance and productivity of seagrasses and macroalgae in Florida Bay, *Bull. Mar. Sci.*, *44*, 292–311.